Covalently porphyrin-functionalized single-walled carbon nanotubes: a novel photoactive and optical limiting donor–acceptor nanohybrid†

Zhen Guo,[a] Feng Du,[b] Dongmei Ren,[a] Yongsheng Chen,*[b] Jianyu Zheng,*[a] Zhibo Liu[c] and Jianguo Tian[c]

Received 16th February 2006, Accepted 25th May 2006
First published as an Advance Article on the web 13th June 2006
DOI: 10.1039/b602349e

Novel covalently porphyrin-functionalized single-walled carbon nanotubes (SWNTs) have been synthesized by the reaction of SWNTs with *in situ* generated porphyrin diazonium compounds. The resulting nanohybrid was characterized by spectroscopic (UV-Vis-NIR, FTIR and Raman) and microscopic (TEM and AFM) methods. The Raman and absorption spectroscopy data showed that the electronic properties of the modified tubes were mostly retained, without damaging their one-dimensional electronic properties. The fluorescence from the porphyrin moiety was almost completely quenched by SWNTs, indicating that the unique direct linkage mode facilitated the effective energy and electron transfer between the excited porphyrin moiety and the extended π-system of SWNTs. This novel nanohybrid material also exhibited excellent optical limiting properties.

Introduction

Single-walled carbon nanotubes (SWNTs) have attracted much attention since they were discovered by Ijima in 1993.[1] Due to the rigid rod-like structure and highly delocalized, extended π-electron systems of SWNTs, these one-dimensional nanowires have many unique mechanical and electronic properties.[2] Porphyrins are stable natural functional dyes with a large extinction coefficient in the visible light region, predictable rigid structures, and prospective photochemical electron-transfer ability, and have been widely studied for various photo-harvesting and photoelectronic devices.[3] Since Nakashima and co-workers reported the first porphyrin–nanotube nanocomposite formed due to van der Waals forces,[4] several non-covalent systems have been investigated for SWNT–porphyrin hybrid materials in the last two years for various molecular photoelectronic applications; these have been constructed using π–π and van der Waals interactions,[4–6] polymer wrapping[7] and electrostatic interactions.[8] However, studies of the covalent incorporation of light-harvesting porphyrin chromophores with the extended π-system of SWNTs have been limited. Recently, Ya-Ping Sun *et al.* and Durairaj Baskaran *et al.* have reported porphyrin-functionalized SWNTs bound covalently with an ester linkage,[9] in which SWNTs bearing carboxylic groups on the sidewall and at the terminal were esterified with hydroxyl porphyrins. In this article, we report the synthesis and characterization of a novel covalently porphyrin-functionalized SWNT nanohybrid (SWNTs–TPP, Schemes 1 and 2) constructed with a unique

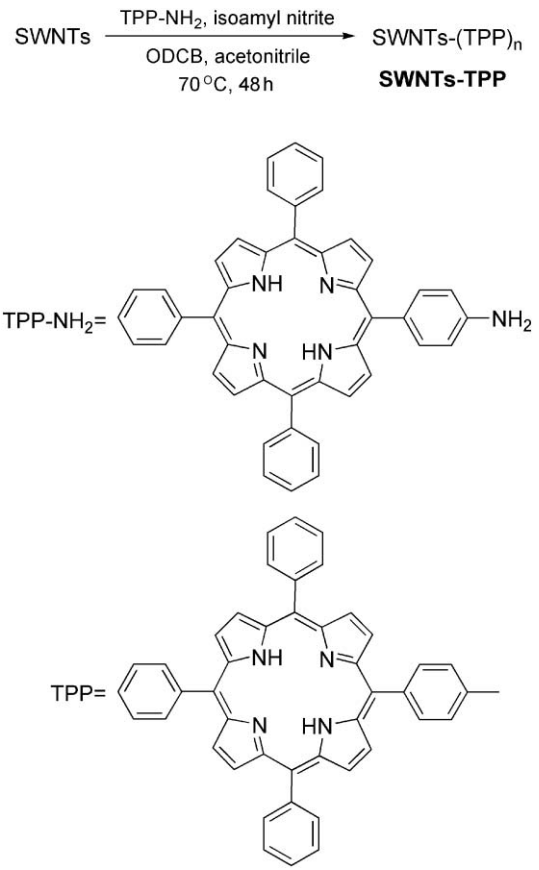

Scheme 1 Preparation of SWNTs–TPP.

[a]*State Key Laboratory and Institute of Elemento-Organic Chemistry, Nankai University, Tianjin 300071, China. E-mail: jyzheng@nankai.edu.cn; Fax: +86 (22)-2350-5572; Tel: +86 (22)-2350-5572*
[b]*Center for Nanoscale Science and Technology and Key Laboratory for Functional Polymer Materials, Institute of Polymer Chemistry, College of Chemistry, Nankai University, Tianjin 300071, China. E-mail: yschen99@nankai.edu.cn; Fax: +86 (22)-2350-0693; Tel: +86 (22)-2350-0693*
[c]*The Key Laboratory of Advanced Technique and Fabrication for Weak-Light Nonlinear Photonics Materials, Ministry of Education and TEDA Applied Physical School, Nankai University, Tianjin 300457, China*
† Electronic supplementary information (ESI) available: FTIR spectra of SWNTs–TPP, Raman and UV-Vis-NIR spectra of control experiments, fluorescence spectra of TPP and SWNTs–TPP, and the absorbance changes of the porphyrin moiety after adding HCl. See DOI: 10.1039/b602349e

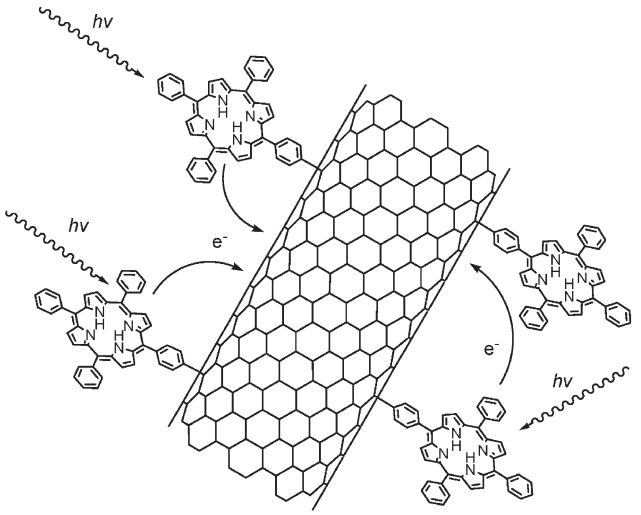

Scheme 2 Schematic representation of part of the structure of SWNTs–TPP.

direct linkage using *in situ* generated diazonium compounds. The steady- and excited-state interactions between porphyrin and SWNTs were probed by spectroscopic methods. Optical limiting behavior was further investigated with nanosecond laser pulses. The results indicate that these novel porphyrin-functionalized SWNTs show significantly better optical limiting performance than SWNTs and C_{60}.

Experimental

Instruments and measurements

UV-Vis-NIR spectra were obtained with a JASCO V-570 spectrometer, and UV-Vis spectra were recorded on a VARIAN Cary 300 spectrophotometer using a quartz cell with a path length of 10 mm. Fluorescence spectra were obtained with a VARIAN Cary Eclipse fluorimeter. FTIR spectra were obtained with a BRUKER TENSOR 27 instrument. All IR samples were prepared as pellets using spectroscopic grade KBr. Raman spectra were measured by a Renishaw inVia Raman microscope at room temperature with the 514 nm line of an Ar ion laser as an excitation source. ^{1}H NMR spectra were recorded on a Bruker (300 MHz) spectrometer using TMS as the internal standard. Separations of SWNTs from the impurities were performed with a centrifuge (Eppendorf 5810R), and filtration was performed through a nylon membrane (Whatman International Ltd, England/MAGNA, 0.2/0.1 μm, 47 mm). Water bath sonication was performed with a KQ-400KDE (400 W, 40 kHz, Kunshan Sonicator Instrument Co. Inc.) sonicator. For thermogravimetric analysis (TGA), a NETZSCH STA 409PC instrument was used, and all samples (typically *ca.* 10 mg) were heated in an alumina pan in dry argon or air flow (20 sccm) to 960 °C at a rate of 2 °C min^{-1}. Transmission electron microscope (TEM) images were obtained on a FEI TECNAI-20 instrument operated at 100 kV. Sample preparation involved sonicating materials in DMF for 2 h and dropping the resulting suspension onto carbon-coated copper grids. Atomic force microscopy (AFM) images were obtained on a Nanoscope IV (Digital Instruments Inc.) using tapping mode with a Si cantilever. The sample solution (10 μL) was dropped onto freshly cleaved mica and dried in vacuum for 10 h prior to AFM imaging. Column chromatography was performed with silica gel (100–200 mesh, Qingdao Haiyang Chemical Co., Ltd, China).

Optical limiting experiments were preformed with linearly polarized 5 ns pulses at 532 nm generated from a frequency-doubled Q-switched Nd:YAG laser. The spatial profiles of the pulses were of nearly Gaussian form after the spatial filter. The pulses were split into two parts. The reflected pulse was used as reference, and we focused the transmitted pulse onto the sample by using a 150 mm focal length lens. The sample was placed at the focus where the spot radius of the pulses was 25 $\pm$ 2 μm. The reflected and transmitted pulse energies were measured simultaneously with two energy detectors (Molectron J3S-10). C_{60} was employed as a standard. For comparison, all of the sample concentrations were adjusted to have same linear transmittance of 75% at 532 nm in 5 mm quartz cells.

Materials

The SWNT sample was produced by using the arc-discharge method with NiO/Y_2O_3 as catalyst using our previously reported procedure.[10] According to the established relationship between the radial breathing mode (RBM) frequency with the tube diameter,[11] individual tubes have a diameter range of 1.4–1.7 nm, which is larger than HiPco SWNTs.[12] Acetonitrile and *o*-dichlorobenzene (ODCB) were distilled from calcium hydride before use. *N*,*N*-Dimethylformamide (DMF) was distilled freshly from anhydrous calcium sulfate. THF, toluene and benzene were dried and distilled from sodium. All other chemicals (AR) obtained from commercial sources were used without further purification.

Purification of SWNTs

1.0 g SWNT raw soot was first heated in an air current with a flow rate of *ca.* 800 sccm at 350 °C for 3 h. The remaining soot was sonicated in 200 mL 36% (w/w) hydrochloric acid for 4 h and then refluxed for 5 h. The mixture was centrifuged and the supernatant acid was decanted off. The sediment was washed with de-ionized water three times and then ultrasonically dispersed into 400 mL 0.2% benzalkonium chloride solution. The solution was transferred to poly(tetrafluoroethylene) centrifuge tubes and centrifuged at 4000 rpm for 30 min. The supernatant solution was filtrated with nylon membrane disc filters (0.2 μm) under vacuum, washed extensively with de-ionized water and dried under vacuum. About 100 mg of purified SWNTs were obtained.

The air oxidation and acid treatment purification process[8b,13] removed most of the impurities (amorphous carbon and metal catalyst) as evidenced by the low end-residue after the TGA heating process in air (see the Results and discussion section).[14] The metal oxide catalyst residue (NiO/Y_2O_3) was reduced from *ca.* 33 wt% to less than 9 wt%, which corresponds to 1.8 at% of metals in purified SWNTs. The tubes obtained have a relative carbonaceous purity of >90 wt%.[15]

Estimatation of the effective extinction coefficient of SWNTs and SWNTs–TPP

The solutions of SWNTs were prepared as follows: Purified SWNTs (2.6 mg) were sonicated in DMF (100 mL) for 30 min to give a homogeneous gray–black solution of concentration 26 mg L^{-1}. The resulting solution, with stability for periods up to several days, was visually non-scattering and was used as a SWNT stock solution. Samples with other concentrations (17, 13, 8.7, 4.4, 1.6 and 0.84 mg L^{-1}) were prepared by diluting the stock solution with DMF and sonicating for an additional 5 min. Absorption spectra were recorded immediately after preparation of the solution. Samples of SWNTs–TPP were prepared using the same procedure.

Preparation of porphyrin

5-(*p*-Aminophenyl)-10,15,20-triphenylporphyrin (TPP-NH_2) was synthesized according to a report in the literature.[16]

Preparation of porphyrin-functionalized SWNTs (SWNTs–TPP) (Scheme 1)

6.3 mg of purified SWNTs was sonicated for 4 h in 7.5 mL *o*-dichlorobenzene (ODCB). To this suspension was added 20 mg (0.032 mmol) of 5-(*p*-aminophenyl)-10,15,20-triphenylporphyrin (TPP-NH_2) in 2.0 mL of acetonitrile. After transfer to a septum-capped flask and bubbling with nitrogen for 10 min, 10 μL (0.074 mmol) of isoamyl nitrite was quickly added and the suspension was stirred in the dark at 70 °C under nitrogen for 48 h. Another 100 mg (0.16 mmol) TPP-NH_2 and 50 μL (0.37 mmol) isoamyl nitrite were added in 5 portions (total 5 × 20 mg TPP-NH_2 and 5 × 10 μL isoamyl nitrite) during this period to ensure a high degree of functionalization. After cooling to room temperature, the suspension was diluted with 10 mL *N*,*N*-dimethylformamide (DMF), filtered over a nylon membrane (0.1 μm), and washed extensively with DMF. Sonication and redispersion was repeated in DMF and then in ether to remove the adsorbed porphyrin and solvent. The final product was collected by filtration over a nylon membrane (0.1 μm) and dried in vacuum at 80 °C for 10 h to give the modified SWNTs as a black powder (5.8 mg).

Results and discussion

Synthesis and characterization

Functionalization of SWNTs using *in situ* generated aryl diazonium compounds was developed by Tour and co-workers.[17] This method avoids the use of unstable aryl diazonium salts. In the synthesis of SWNTs–TPP, isoamyl nitrite was used to oxidize the amino group on 5-(*p*-aminophenyl)-10,15,20-triphenylporphyrin (TPP-NH_2) to a diazo group and release N_2 to form an aryl radical. This active radical reacts with the double bonds on the walls of SWNTs to generate the functionalization.[18] Thus the porphyrin is covalently attached to the surface of the SWNTs with a benzene ring between these two moieties. The Raman spectra of porphyrin-functionalized SWNTs (SWNTs–TPP) was significantly different than that of unfunctionalized SWNTs (Fig. 1). Relative to the tangential

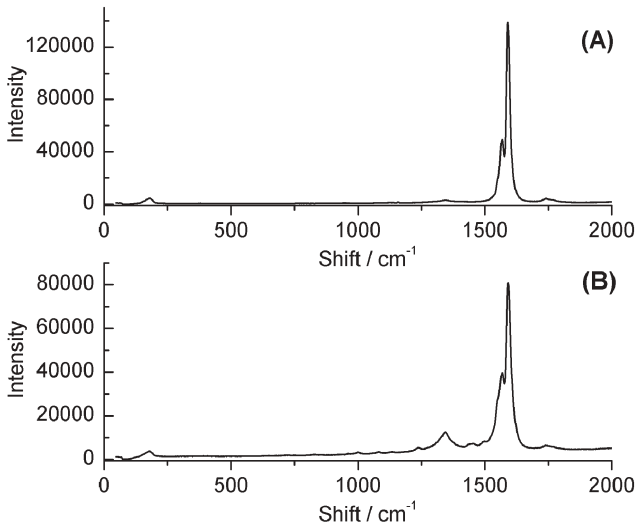

Fig. 1 Raman spectra (514 nm excitation) of SWNTs, (A) before and (B) after TPP functionalization.

mode at ~1590 cm^{-1} (G-band), the intensity of the disorder mode at ~1350 cm^{-1} (D-band) increased significantly, and the ratio of the peak intensities of the tangential mode and the disorder mode decreased from *ca.* 30–40 to *ca.* 10, indicating the conversion of sp^2 carbons to sp^3 carbons on the SWNT surface due to the functionalization. The disorder mode involves the resonance-enhanced scattering of an electron *via* phonon emission by a defect that breaks the basic symmetry of the graphene plane.[19] Thus the ratio of peak intensities of the tangential mode and the disorder mode can reflect the relative amount of sp^3 carbon on SWNTs, and can be used to estimate the degree of functionalization.[17a] The FTIR spectrum of SWNTs–TPP (see ESI, Fig. S1†) exhibit the characteristic porphyrin absorptions at 3302, 1636, 1536, 1467, 1416, 1275, 1199, 798 and 691 cm^{-1}. The absorption band at 3302 cm^{-1} can be assigned to the stretching vibration of the pyrrole N–H of the porphyrin. The bands at 1275 and 1199 cm^{-1} can be assigned to the stretching vibration of the pyrrole C–N bond. A series of strong absorption bands from 1650 to 1400 cm^{-1} can be attributed to the stretching vibration of the phenyl C=C bonds of the porphyrin, and the bands at 798 and 691 cm^{-1} can be attributed to the out-of-plane bending vibration of the phenyl C–H bonds. These IR data indicate the existence of the porphyrin moieties on functionalized SWNTs.

The room temperature UV-Vis-NIR absorption spectrum of SWNTs–TPP in DMF (Fig. 2) showed a Soret band at 422 nm and broad bands of van Hove singularities at ~700, ~1000 and ~1800 nm, corresponding separately to porphyrin and SWNTs. Compared to the absorption spectrum of 5,10,15,20-tetraphenylporphyrin (TPP) in DMF, the spectrum of SWNTs–TPP shows a 5 nm red-shift of the Soret band (417 nm to 422 nm) and 4–7 nm red-shift of the Q-bands (*e.g.* 514 nm to 521 nm, 647 nm to 651 nm), with notable broadening of the Soret band for the porphyrin moiety. This reflects that the covalent bonding to SWNTs causes some alteration of the electronic states of TPP, and that there is notable electronic communication between the two π-systems of SWNTs and TPP in the ground state.[5c] Noncovalently

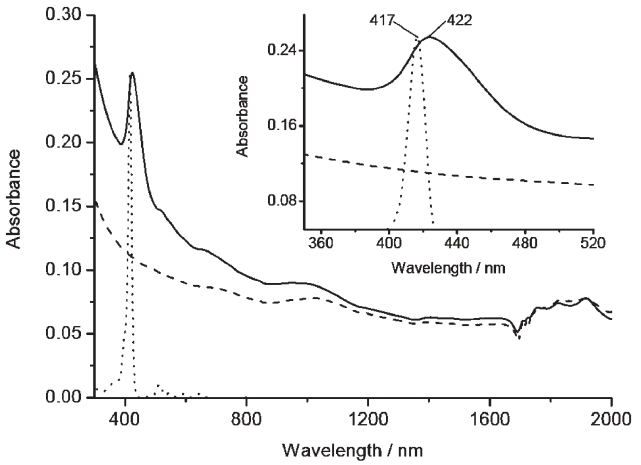

Fig. 2 UV-Vis-NIR spectra of SWNTs–TPP (solid line), SWNTs (dashed line) and TPP (dotted line) in DMF. The inset shows the Soret-band region in more detail.

attached porphyrins on SWNTs do not cause shift or broadening of the Soret band except when there are other strong interactions (*e.g.* electrostatic Coulomb force), as previously reported,[4–9,20] and so the phenomenon observed here gives strong support for the covalent attachment of porphyrins on SWNTs. Van Hove singularities of SWNTs are usually lost after a high degree of covalent functionalization, leaving no discernible peaks in the near-IR spectrum, reflecting the disruption of the extended conjugated π-network of the sp^2-hybridized nanotubes.[17d,21] However, the characteristic van Hove singularities in our SWNT–TPP nanohybrid are basically retained, indicating that our functionalization did not severely damage the structure of the SWNT bundles,[22] and that the π-conjugation electron structure of the nanotubes has been mostly preserved.[23]

Two control experiments were also carried out to prove the covalent attachment of porphyrin on SWNTs: control experiment A, where the reactant, 5-(*p*-aminophenyl)-10,15,20-triphenylporphyrin (TPP-NH_2), was replaced by 5,10,15,20-tetraphenylporphyrin (TPP), and B, where isoamyl nitrite was not employed. The Raman spectra of the SWNTs obtained from these two control experiments (see ESI, Fig. S2†) were almost identical to SWNTs, and no disorder mode increase was observed. The UV-Vis-NIR spectrum of SWNTs obtained in control A (see ESI, Fig. S3A†) showed no characteristic absorptions of porphyrin from 400 nm to 700 nm, and that from control B (see ESI, Fig. S3B†) only showed a very weak Soret band absorption with no peak shift. These control experiments results clearly indicate that SWNTs–TPP were formed by direct covalent bonding of TPP directly onto the walls of the SWNTs.

Thermogravimetric analysis (TGA) has been used widely to investigate the covalent functionalization of SWNTs.[24,25] The TGA curve of purified SWNTs showed low end-residue (9 wt%) compared to unpurified SWNTs (33 wt%), indicating that most of the metal oxide catalyst have been removed (Fig. 3A, traces 1 and 2). Upon heating of SWNTs–TPP in air, there was a continuous mass loss over a wide temperature range, 200 to 600 °C, and the weight loss curve shows no clear

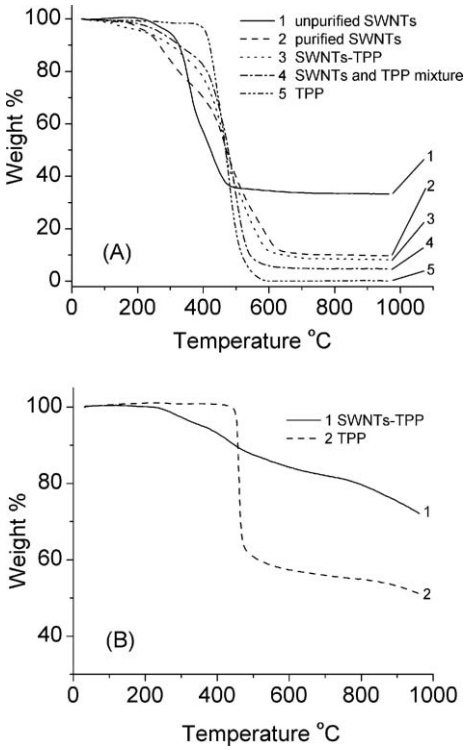

Fig. 3 (A) TGA thermograms of (1) unpurified SWNTs, (2) purified SWNTs, (3) SWNTs–TPP, (4) a mixture of SWNTs and TPP in a 1 : 1 weight ratio made from ODCB solution and (5) TPP, in air. (B) TGA thermograms of (1) SWNTs–TPP and (2) TPP, in argon.

weight loss steps (Fig. 3A, trace 3). This is consistent with earlier reports for other covalently functionalized SWNTs.[24] In a control TGA experiment using a sample with a 1 : 1 weight ratio of purified SWNTs and TPP mixed by sonicating in *o*-dichlorobenzene, a major weight loss in a limited range of 400 to 540 °C was observed (Fig. 3A, trace 4). This limited range and pattern are similar to pure TPP, shown in Fig. 3A (trace 5), but very different to that of covalently porphyrin-modified SWNTs (Fig. 3A, trace 3). These results provided further evidence for the covalent sidewall functionalization of SWNTs. The TGA weight loss of modified SWNTs in argon has been widely used to estimate the content of functional groups on SWNTs.[17c,19,25] Fig. 3B (trace 1) shows the TGA of SWNTs–TPP in argon. The steady mass loss up to 28% from 250 °C to above 960 °C without a plateau is a pattern typical of sidewall functionalization,[25] reflecting a stepwise detachment of covalently linked porphyrin moieties from SWNT sidewalls. Unlike other relatively small organic groups, TPP does not lose its whole mass in argon due to the carbonization effect (Fig. 3B, trace 2),[17c,19] so it would not be reliable to calculate the content of TPP using the weight loss of SWNTs–TPP. However, we can still argue that the content of TPP in SWNTs–TPP should be more than 28% from the observed weight loss at 960 °C.

Solution-phase UV-Vis-NIR spectroscopy has been reported to demonstrate a linear relationship between the absorbance and the relative concentrations of SWNTs in different solvents, obeying Beer's law at low concentrations, and has been used to determine the solubility of SWNTs.[26] The absorption spectra

of solutions of SWNTs and SWNTs–TPP with different concentrations were measured, and the absorption values at 1000 nm were plotted against concentrations to get a standard curve (in mg L^{-1}, Fig. 4 and the inset). On the basis of the applicability of Beer's law, we can estimate the effective extinction coefficient of SWNTs and SWNTs–TPP from the slope of the linear least-squares fit to be 0.026 L mg^{-1} cm^{-1} and 0.010 L mg^{-1} cm^{-1} respectively, with an R value of 0.999. The absorbance of solutions of SWNTs and SWNTs–TPP at different wavelengths was well in line with the relative concentrations, thus indicating that they have been homogeneously dispersed in the solvent.[27] As the absorption coefficient of SWNTs varies due to different existence states and different production methods,[28] the literature data are very inconsistent, and so we did not use it to estimate the weight content of TPP in SWNTs–TPP from the extinction coefficient obtained. However, this method can be used to evaluate the solubility of SWNTs and SWNTs–TPP separately. Saturated solutions of these two materials in DMF were diluted to a concentration at which the absorption at 1000 nm matches the standard curve. The solubilities could then be calculated to be 56 mg L^{-1} and 211 mg L^{-1} respectively. The much-enhanced solubility indicates that modification by porphyrin helps to disperse SWNTs in the solvent, which may be caused by exfoliating of nanotube bundles. This is in accordance with the reduced bundle size observed from TEM images (*vide infra*).

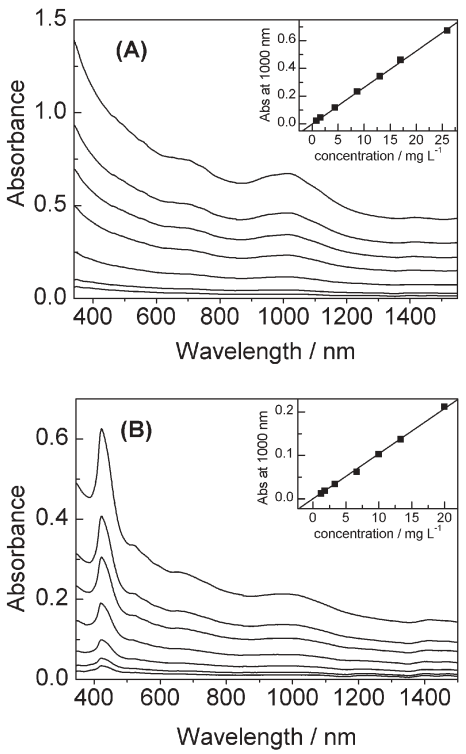

Fig. 4 Absorption spectra of (A) SWNTs in DMF (concentrations are 26, 17, 13, 8.7, 4.4, 1.6 and 0.84 mg L^{-1} respectively), and (B) SWNTs–TPP in DMF (concentrations are 20, 13, 10, 6.7, 3.3, 1.8 and 1.3 mg L^{-1} respectively). Shown in the insets are the plots of optical density at 1000 nm *versus* concentration. The straight lines are a linear least-squares fit to the data.

Microscopy analysis

Fig. 5 shows the tapping mode AFM image of a small bundle of SWNTs–TPP. As is shown in the height profile in Fig. 5B, the diameter of the modified SWNTs does not appear uniform along their lengths, and the rough tube surface indicates the existence of porphyrins. The height of the dark gray arrow at the trough of the SWNT surface is 4.25 nm above that of the arrow at the horizontal line, which is in line with the bundle of SWNTs. The height of the light gray arrow at the wave crest is 7.33 nm, and the height difference between this arrow and the arrow at the trough of the surface is 3.08 nm, which is larger than the diameter of a porphyirn molecule (*ca.* 1 nm). One possible reason for this result is that porphyrins can be attached to both sides of either a single nanotube or a bundle. It is worthy of note that a clear pattern of periodicity appears in the AFM height profile analysis (Fig. 5B) and that the average distance between the peaks is roughly 100 nm. This interesting periodicity, though similarly reported by Kruse and co-workers,[29] remains to be understood.

Transmission electron microscopy (TEM) allowed direct imaging of SWNT samples at the level of individual SWNTs or their thin bundles.[30] Fig. 6 shows the typical surface morphology of SWNTs before and after porphyrin functionalization. As shown in the image of Fig. 6A, the relatively clear and smooth SWNT surface became bumpy after porphyrin functionalization. The inset images of Fig. 6 show two individual SWNTs. Clearly, the sidewalls of the SWNTs was significantly roughened by the coverage of soft material, indicating the presence of porphyrin attached to the SWNT surface.[14,25b,25c,31] Although information obtained from TEM and AFM should not be over-emphasized, these methods still provide complementary evidence for porphyrin covalent functionalization.

Fluorescence and electronic absorption investigations

In order to probe excited-state interactions of porphyrins and SWNTs, fluorescence spectra of SWNTs–TPP and TPP were compared. Upon excitation of the porphyrin moiety at the Soret band, the solution of SWNTs–TPP exhibited 97% quenching of fluorescence emission at 651 nm and 717 nm (Fig. 7). Even when the absorption of SWNTs was subtracted from the absorbance of SWNTs–TPP at the Soret band, >90% of the fluorescence was quenched (see ESI, Fig. S4†). Similar quenching (98–99%) was also observed at other excitation wavelengths (400, 422, 514, 521 and 550 nm, see ESI, Fig. S5†). The observed luminescence quenching indicates that there is a strong interaction between the excited state of the porphyrin and SWNTs.[4,32] Possible pathways for the deactivation of excited porphyrins may be attributed to two competitive processes, energy transfer (ET) and photoinduced electron transfer (PET). Because the emission of TPP (651 nm and 717 nm) overlaps with the absorption of SWNTs, singlet–singlet energy transfer from TPP to SWNT is in principle possible.[27a] Nevertheless, the significant decrease of the fluorescence quantum yield of SWNTs–TPP with increasing solvent polarity (Table 1) indicates that the quenching process in our SWNT–TPP nanohybrid is dominated by the excited-state electron transfer, as the energy transfer commonly does

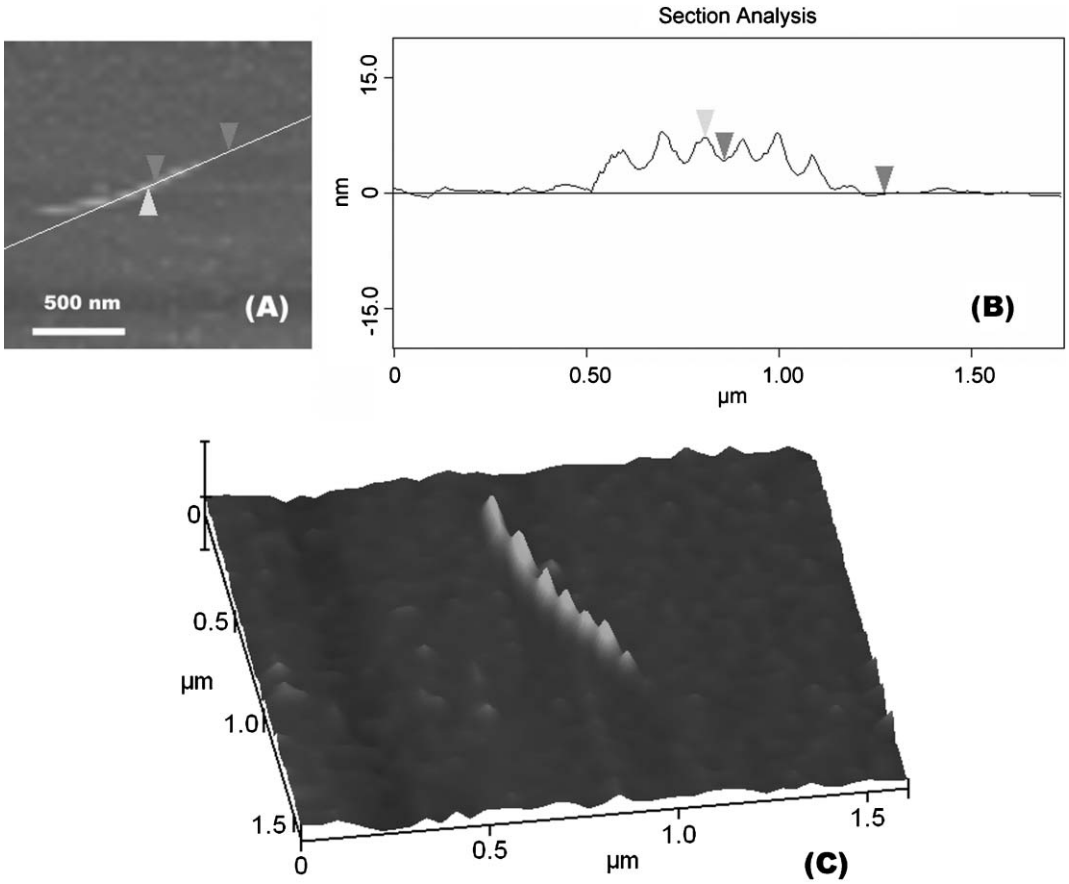

Fig. 5 (A) AFM image of a small individual bundle of SWNTs–TPP on a mica surface. (B) AFM height profile taken along the length of SWNT axis as shown by straight line in (A). (C) AFM 3-D topographic view corresponding to (A).

not depend on solvent polarity while the electron transfer tends to be sensitive to medium effects.[9a,33,34] Molecular orbital theory and experimental results have shown that closed-cage carbon structures such as fullerenes and carbon nanotubes are favorable electron acceptors because of their unique π-electron system.[35] Thus, after photoexcitation, the internal donor–acceptor interaction between the two moieties of TPP and SWNTs in our SWNT–TPP nanohybrid causes a charge transfer from the photoexcited singlet porphyrin moiety to SWNTs, and this energy gets released.[8b,9] Considering the direct covalent attachment of porphyrin moieties on SWNTs in this SWNT–TPP nanohybrid and the reduced mobility of SWNT bundles,[36] the conformations of pre-associated donor and acceptor will affect the efficiency of static quenching.[9a,37] Previously reported porphyrin–nanotube hybrids linked by flexible chains[9a] showed fluorescence quenching, as the flexible chain allowed the porphyrin to face the nanotube surface, which facilitated the through-space intramolecular energy transfer, but when the linkage chains became shorter, no fluorescence quenching occurred.[9a] In our SWNT–TPP nanohybrids, the effective intramolecular quenching may be explained by the extended conjugated π-system of SWNTs and the porphyrin mediated by a through-bond mechanism, due to the unique direct linkage mode of the two moieties.[33,38]

The ground-state interactions of porphyrins and SWNTs were probed by comparing the absorption spectrum of the covalent SWNT–TPP nanohybrid and that of a simple mixture of solubilized SWNTs and TPP (SWNTs/TPP). A DMF solution of TPP (8.5×10^{-7} mol L^{-1}) was titrated with SWNTs, and Fig. 8 shows how the absorption spectrum of TPP changes upon addition of increasing concentrations of SWNTs. The obtained spectra are a simple sum of the spectra of the SWNTs and TPP. No red-shift or broadening of the Soret band were observed, as in the spectrum of SWNTs–TPP shown in Fig. 2. This revealed that the relatively weak intermolecular interactions due to π–π stacking and van der Waals forces between the two moieties did not disturb the electronic structure of the porphyrin at the steady state. However, for SWNTs–TPP, the π-delocalization along the bridge may enhance the electronic interaction and cause changes in the absorption spectrum, as shown in Fig. 2. This is in accordance with the reported result that mixtures of SWNTs and non-covalently adsorbed porphyrins do not show a major shift of the Soret band when there are not additional strong interactions between them.[4–9,20,41]

Solution stability investigations

The solution stabilities of covalent and non-covalent systems were different. Although the DMF solution of SWNTs with non-covalently adsorbed porphyrins was stable for carrying out spectroscopic and microscopic measurements,[6b] visible particles appeared after *ca.* 6 h. However, the solution of

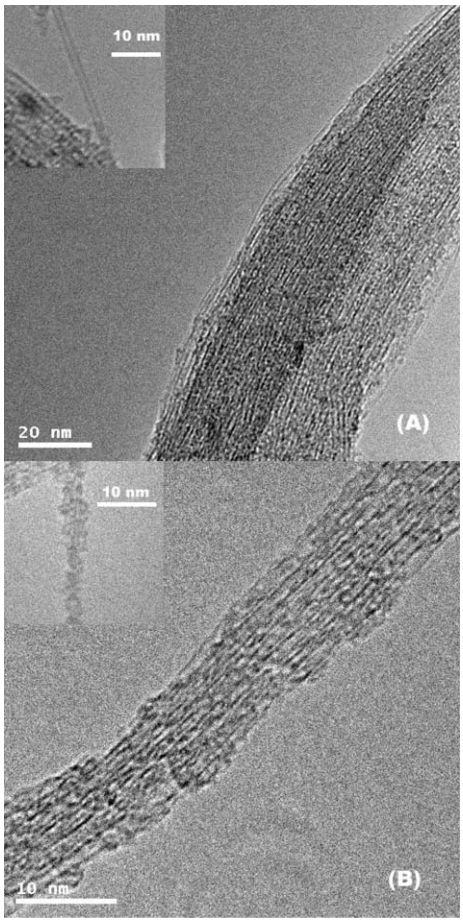

Fig. 6 TEM images of: (A) purified SWNTs and (B) functionalized SWNTs. The insets show zoomed-in pictures of individual SWNTs.

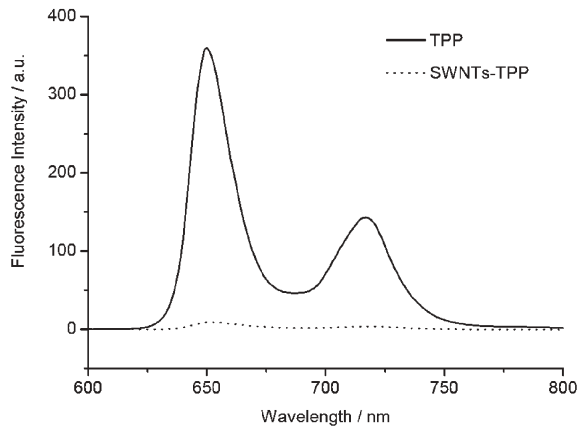

Fig. 7 Fluorescence spectra of DMF solutions of TPP (top), SWNTs–TPP (bottom) with normalization of the absorbance of the Soret band excitation wavelength to the same value (0.255).

SWNTs–TPP in DMF was stable for periods up to several days. Just as reported by Prof. Smalley and co-workers,[26a] the boundary between SWNT solution and suspension in organic solvents is somewhat ambiguous. The solutions are metastable systems, and most of the SWNTs exist as ropes and bundles with a small amount existing as individual tubes, though there were no visible particles. Our observed Tyndall effect (Fig. 9)

Table 1 Fluorescence quantum yields of SWNTs–TPP in solvents of different polarity

Solvent	Dielectric constant[a]	Relative Φ_f
Toluene	2.43	1.0[b]
THF	7.47	0.50
DMF	37.06	0.28

[a] From ref. 39. [b] Measured at 298 K. Solutions were deoxygenated by purging with N_2 before quantum yields were determined. The quantum yield is 0.024 with reference to that of TPP (in benzene, Φ_f = 0.13). The quantum yields have been corrected for the difference in solvent refractive index relative to that of benzene.[40]

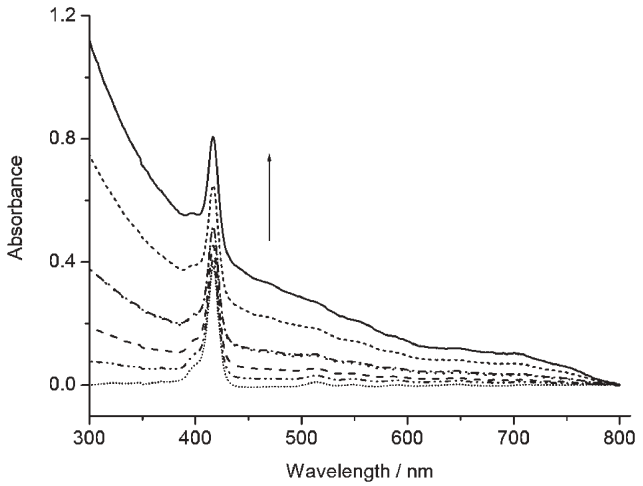

Fig. 8 Absorption spectra of TPP solution (8.5×10^{-7} mol L^{-1}) titrated against a SWNT solution in DMF normalized to zero absorption at 800 nm.

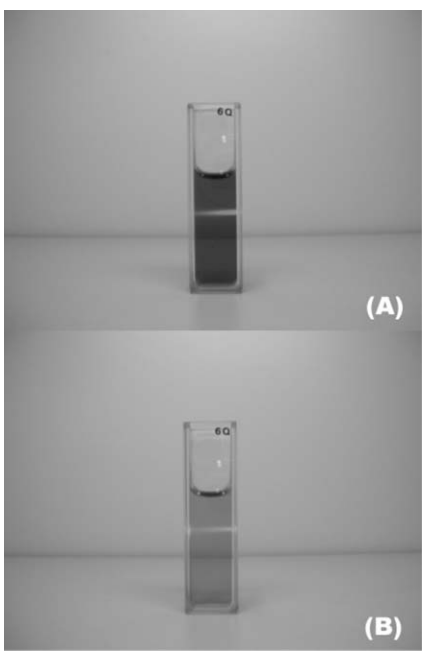

Fig. 9 (A) Solution of SWNTs (26 mg L^{-1}) and (B) solution of SWNTs–TPP (20 mg L^{-1}) in DMF with a laser beam at 650 ± 10 nm.

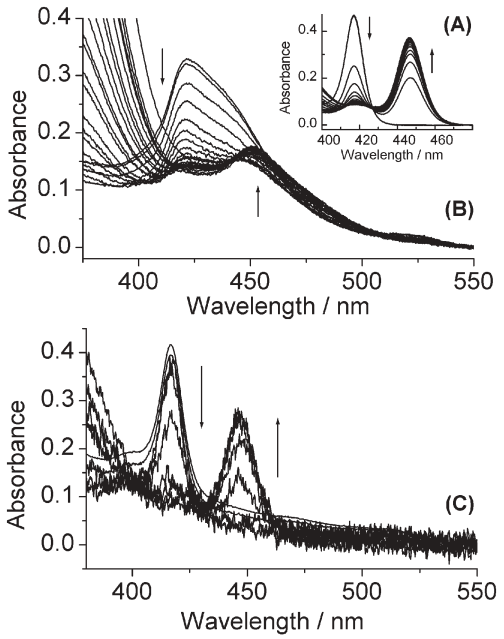

Fig. 10 Changes in absorption spectra of (A) TPP, (B) SWNTs–TPP and (C) SWNTs/TPP after the addition of increasing amounts of 0.46 N HCl (aq.) (normalized to zero absorption at 480 and 550 nm).

does indicate that the solutions of SWNTs–TPP are still some kind of colloid.[26a,42]

The stability of SWNTs–TPP was further studied by the titration of electrolytes such as hydrochloric acid to accelerate the colloid coagulation.[6a] Fig. 10 shows the absorption spectra changes of TPP, SWNTs–TPP and SWNTs/TPP after adding hydrochloric acid until all the porphyrin moieties were protonated (for an absorbance maxima plot of the titration, see ESI, Fig. S6†). The peaks at *ca.* 450 nm were the absorption of the protonated porphyrin moiety. When 2 μL of 0.46 N HCl solution was added to the solution of the mixture of SWNTs/TPP, visible black deposits appeared immediately, and the absorption spectrum became 'bumpy' because of the scattering caused by these particles. When adding HCl to a solution of SWNTs–TPP, no visible particles were observed even after all the porphyrin had been completely protonated. Solutions used for optical limiting measurements (see below) also showed the same results. A precipitate was observed for the solution of SWNTs after 24 h of laser irradiation, but the solution of SWNTs–TPP remained clear. Clearly, porphyrins covalently attached to SWNTs–TPP help to disperse the SWNTs in the solvent and sustain the stability of the resulting colloid to environmental changes.

Optical limiting properties of SWNTs–TPP

Optical limiters are materials that exhibit high transmittance for low-intensity light, and attenuate intense optical beams.[43] They can be used to protect optical sensors, *e.g.* eyes or CCD cameras, from possible damage caused by intense laser pulses, and have potential application in the field of optical switching and other areas. Optical limiting properties of carbon nanotubes have been studied extensively in recent years due to their excellent linear transmittance and broadband applicability.[44] Both SWNT and MWNT suspensions have been reported to be good optical limiters with a non-linear light-scattering mechanism.[44,45] However, optical limiting properties have hardly been studied for functionalized SWNTs with light-harvesting chromophores. In particular, functionalized SWNTs with reverse saturation absorption (RSA) groups, such as porphyrins, have not been studied for their optical limiting response. Porphyrins are well known for their excellent light-harvesting properties and remarkable non-linear optical (NLO) behavior, because of the polarizable large π-electron conjugation over their two-dimensional molecular structure.[3,46] So it would be both interesting and important to investigate the optical limiting properties of the hybrid system of SWNTs with porphyrins.

Fig. 11 shows the optical limiting properties of C_{60} (in toluene), and SWNTs, TPP and SWNTs–TPP (in DMF). The optical limiting properties of the suspensions of these materials were investigated using 532 nm pulsed laser irradiation, and C_{60} was employed as a standard. For comparison, the concentrations of all samples were adjusted to give 75% linear transmittance at 532 nm. At low input, the output fluence rises linearly with the increase of input fluence, and after a certain threshold value (*ca.* 40 J cm^{-2}) the output fluence of SWNTs–TPP tends to reach a constant, while the output for SWNTs, TPP and C_{60} continues to increase. When the fluence of the laser pulses increases to 95 J cm^{-2}, the output fluence from SWNTs–TPP is 3.7 J cm^{-2}, which is much less than the output of the others. Therefore, SWNTs–TPP show much better optical limiting properties compared with the benchmark material (C_{60}) and the individual components (TPP and SWNTs). Considering the donor–acceptor property of this nanohybrid in the excited state, we believe that the much-enhanced optical limiting performance of SWNTs–TPP is due to the charge-separated excited state produced by photo-induced electron transfer from the electron-donating TPP moiety to the electron-accepting SWNTs.[47] Further studies to better understand the mechanism and the structure–property correlations are currently in progress.

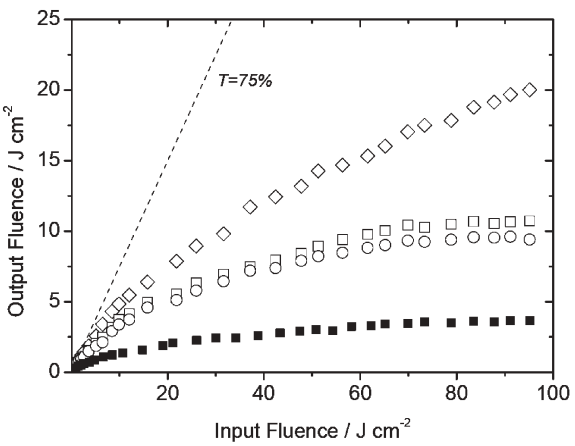

Fig. 11 Optical limiting responses (to 5 ns, 532 nm optical pulses) of: C_{60} (□) in toluene, and TPP (◇), SWNTs (○) and SWNTs–TPP (■) in DMF.

Conclusion

In summary, we have synthesized novel covalently porphyrin-functionalized SWNTs. Raman, FTIR, UV-Vis-NIR absorption spectra and controlled experiments confirm the covalent functionalization of the sidewalls. This was also supported by microscopic (TEM and AFM) and TGA studies. The considerable porphyrin attachment significantly improved the solubility and dispersion stability of the SWNTs in organic solvents. In this donor–acceptor nanohybrid, fluorescence of photoexcited porphyrin was effectively quenched through intramolecular electron transfer process. More significantly, these novel covalently modified SWNTs show superior optical limiting effects for nanosecond laser pulses, significantly better than SWNTs and C_{60}. Thus, with its direct rigid linkage, this nanohybrid is a theoretically significant and promising candidate for optoelectronic devices, such as optical limiting and solar-energy conversion applications.

Acknowledgements

We thank the Natural Science Foundation of China (Grant No. 20172028 and 20421202), NSF Funding (Grant No. 043803711) from Tianjin City, the Trans-Century Training Program Foundation for the Talents by the State Education Commission (Grant No. 20020048) and the Preparatory Project of the National Key Fundamental Research Program (Grant No. 2004CCA04400) for their generous financial support.

References

1 S. Iijima and T. Ichihashi, *Nature*, 1993, **363**, 603.
2 *Carbon Nanotubes: Synthesis, Structure, Properties and Applications*, ed. M. S. Dresselhaus, G. Dresselhaus and P. Avouris, Springer, Berlin, 2001.
3 (*a*) T. S. Balaban, A. D. Bhise, M. Fischer, M. Linke-Schaetzel, C. Roussel and N. Vanthuyne, *Angew. Chem., Int. Ed.*, 2003, **42**, 2140; (*b*) M.-S. Choi, T. Yamazaki, I. Yamazaki and T. Aida, *Angew. Chem., Int. Ed.*, 2004, **43**, 150.
4 H. Murakami, T. Nomura and N. Nakashima, *Chem. Phys. Lett.*, 2003, **378**, 481.
5 (*a*) G. M. A. Rahman, D. M. Guldi, S. Campidelli and M. Prato, *J. Mater. Chem.*, 2006, **16**, 62; (*b*) H.-P. Li, B. Zhou, Y. Lin, L.-R. Gu, W. Wang, K. A. S. Fernando, S. Kumar, L. F. Allard and Y.-P. Sun, *J. Am. Chem. Soc.*, 2004, **126**, 1014.
6 SWNT-induced J- and H-aggregates of porphyrins: (*a*) J.-Y. Chen and C. P. Collier, *J. Phys. Chem. B*, 2005, **109**, 7605; (*b*) T. Hasobe, S. Fukuzumi and P. V. Kamat, *J. Am. Chem. Soc.*, 2005, **127**, 11884.
7 (*a*) A. Satake, Y. Miyajima and Y. Kobuke, *Chem. Mater.*, 2005, **17**, 716; (*b*) D. M. Guldi, H. Taieb, G. M. A. Rahman, N. Tagmatarchis and M. Prato, *Adv. Mater.*, 2005, **17**, 871.
8 (*a*) D. M. Guldi, G. N. A. Rahman, J. Ramey, M. Marcaccio, D. Paolucci, F. Paolucci, S.-H. Qin, W. T. Ford, D. Balbinot, N. Jux, N. Tagmatarchis and M. Prato, *Chem. Commun.*, 2004, **18**, 2034; (*b*) N. Tagmatarchis, M. Prato and D. M. Guldi, *Physica E (Amsterdam)*, 2005, **29**, 546; (*c*) D. M. Guldi, G. M. A. Rahman, N. Jux, D. Balbinot, U. Hartnagel, N. Tagmatarchis and M. Prato, *J. Am. Chem. Soc.*, 2005, **127**, 9830; (*d*) D. M. Guldi, G. M. A. Rahman, M. Prato, N. Jux, S.-H. Qin and W. Ford, *Angew. Chem., Int. Ed.*, 2005, **44**, 2015; (*e*) D. M. Guldi, G. M. A. Rahman, N. Jux, N. Tagmatarchis and M. Prato, *Angew. Chem., Int. Ed.*, 2004, **43**, 5526; (*f*) D. M. Guldi, *J. Phys. Chem. B*, 2005, **109**, 11432.
9 (*a*) H.-P. Li, R. B. Martin, B. A. Harruff, R. A. Carino, L. F. Allard and Y.-P. Sun, *Adv. Mater.*, 2004, **16**, 896; (*b*) D. Baskaran, J. W. Mays, X. P. Zhang and M. S. Bratcher, *J. Am. Chem. Soc.*, 2005, **127**, 6916.
10 X. Lv, F. Du, Y. Ma, Q. Wu and Y. Chen, *Carbon*, 2005, **43**, 2020.
11 M. S. Dresselhaus, G. Dresselhaus, A. Jorio, A. G. Souza Filho and R. Saito, *Carbon*, 2002, **40**, 2043.
12 M. A. Hamon, M. E. Itkis, S. Niyogi, T. Alvaraez, C. Kuper, M. Menon and R. C. Haddon, *J. Am. Chem. Soc.*, 2001, **123**, 11292.
13 Z.-J. Shi, Y.-F. Lian, F.-H. Liao, X.-H. Zhou, Z.-N. Gu, A.-G. Zhang and S. Iijima, *Solid State Commun.*, 1999, **112**, 35.
14 P. He and M. Bayachou, *Langmuir*, 2005, **21**, 6086.
15 M. E. Itkis, D. Perea, S. Niyogi, S. Rickard, M. Hamon, H. Hu, B. Zhao and R. C. Haddon, *Nano Lett.*, 2003, **3**, 309.
16 W. J. Kruper, Jr., T. A. Chamberlain and M. Kochanny, *J. Org. Chem.*, 1989, **54**, 2753.
17 (*a*) J. L. Bahr and J. M. Tour, *Chem. Mater.*, 2001, **13**, 3823; (*b*) C. A. Mitchell, J. L. Bahr, S. Arepalli, J. M. Tour and R. Krishnamoorti, *Macromolecules*, 2002, **35**, 8825; (*c*) C. A. Dyke and J. M. Tour, *Nano Lett.*, 2003, **3**, 1215; (*d*) C. A. Dyke and J. M. Tour, *J. Am. Chem. Soc.*, 2003, **125**, 1156; (*e*) J. L. Hudson, M. J. Casavant and J. M. Tour, *J. Am. Chem. Soc.*, 2004, **126**, 11158; (*f*) C. A. Dyke and J. M. Tour, *J. Phys. Chem. A*, 2004, **108**, 11151; (*g*) B. K. Price, J. L. Hudson and J. M. Tour, *J. Am. Chem. Soc.*, 2005, **127**, 14867; (*h*) A. K. Flatt, B. Chen and J. M. Tour, *J. Am. Chem. Soc.*, 2005, **127**, 8918; (*i*) C. A. Dyke, M. P. Stewart and J. M. Tour, *J. Am. Chem. Soc.*, 2005, **127**, 4497.
18 C. A. Dyke, M. P. Stewart, F. Maya and J. M. Tour, *Synlett*, 2004, 155.
19 M. S. Strano, C. A. Dyke, M. L. Usrey, P. W. Barone, M. J. Allen, H.-W. Shan, C. Kittrell, R. H. Hauge, J. M. Tour and R. E. Smalley, *Science*, 2003, **301**, 1519.
20 D. M. Guldi, G. M. A. Rahman, S.-H. Qin, M. Tchoul, W. T. Ford, M. Marcaccio, D. Paolucci, F. Paolucci, S. Campidelli and M. Prato, *Chem.–Eur. J.*, 2006, **12**, 2152.
21 D. M. Guldi, G. M. A. Rahman, F. Zerbetto and M. Prato, *Acc. Chem. Res.*, 2005, **38**, 871.
22 J. Chen, H. Liu, W. A. Weimer, M. D. Halls, D. H. Waldeck and G. C. Walker, *J. Am. Chem. Soc.*, 2002, **124**, 9034.
23 Y. Liu, Z. Yao and A. Adronov, *Macromolecules*, 2005, **38**, 1172.
24 S.-H. Qin, D.-Q. Qin, W. T. Ford, J. E. Herrera and D. E. Resasco, *Macromolecules*, 2004, **37**, 9963.
25 (*a*) R. K. Saini, I. W. Chiang, H. Peng, R. E. Smalley, W. E. Billups, R. H. Hauge and J. L. Margrave, *J. Am. Chem. Soc.*, 2003, **125**, 3617; (*b*) L. Zhang, V. U. Kiny, H.-Q. Peng, J. Zhu, R. F. M. Lobo, J. L. Margrave and V. N. Khabashesku, *Chem. Mater.*, 2004, **16**, 2055; (*c*) L. Zeng, L. Zhang and A. R. Barron, *Nano Lett.*, 2005, **5**, 2001.
26 (*a*) J. L. Bahr, E. T. Mickelson, M. J. Bronikowski, R. E. Smalley and J. M. Tour, *Chem. Commun.*, 2001, 193; (*b*) B. Zhao, H. Hu, A.-P. Yu, D. Perea and R. C. Haddon, *J. Am. Chem. Soc.*, 2005, **127**, 8197; (*c*) Y.-J. Qin, L.-Q. Liu, J.-H. Shi, W. Wu, J. Zhang, Z.-X. Guo, Y.-F. Li and D.-B. Zhu, *Chem. Mater.*, 2003, **15**, 3256.
27 We chose DMF as solvent because it can disperse SWNTs well by ultrasonication without appreciable damage to the tubes – see the following references: (*a*) W.-H. Zhu, N. Minami, S. Kazaoui and Y. Kim, *J. Mater. Chem.*, 2003, **13**, 2196; (*b*) S. Niyogi, M. A. Hamon, D. Perea, C. B. Kang, B. Zhao, S. K. Pal, A. E. Wyant, M. E. Itkis and R. C. Haddon, *J. Phys. Chem. B*, 2003, **107**, 8799.
28 (*a*) B. J. Landi, H. J. Ruf, J. J. Worman and R. P. Raffaelle, *J. Phys. Chem. B*, 2004, **108**, 17089; (*b*) H. Paloniemi, T. Ääritalo, T. Laiho, H. Liuke, N. Kocharova, K. Haapakka, F. Terzi, R. Seeber and J. Lukkari, *J. Phys. Chem. B*, 2005, **109**, 8634.
29 K. A. Worsley, K. R. Moonoosawmy and P. Kruse, *Nano Lett.*, 2004, **4**, 1541.
30 T.-J. Park, S. Banerjee, T. Hemraj-Benny and S. S. Wong, *J. Mater. Chem.*, 2006, **16**, 141.
31 Y. Lin, D. E. Hill, J. Bentley, L. F. Allard and Y.-P. Sun, *J. Phys. Chem. B*, 2003, **107**, 10453.
32 I. Robel, B. A. Bunker and P. V. Kamat, *Adv. Mater.*, 2005, **17**, 2458.
33 N. Armaroli, G. Accorsi, J. Gisselbrecht, M. Gross, V. Krasnikov, D. Tsamouras, G. Hadziioannou, M. J. Gómez-Escalonilla, F. Langa, J. Eckerte and J. Nierengarten, *J. Mater. Chem.*, 2002, **12**, 2077.

34 C. Trieflinger, H. Röhr, K. Rurack and J. Daub, *Angew. Chem., Int. Ed.*, 2005, **44**, 6943.
35 P. W. Fowler and A. Ceulemans, *J. Phys. Chem.*, 1995, **99**, 508.
36 (*a*) D.-B. Zhu and F.-S. Wang, *Organic Solids*, Shanghai Scientific & Technical Publishers, Shanghai, 1999; (*b*) Y.-H. Wang, M.-Z. Zhu, X.-Y. Ding, J.-P. Ye, L. Liu and Q.-X. Guo, *J. Phys. Chem. B*, 2003, **107**, 14087.
37 M.-G. Fan, *Basic Fundamentals of Photochemistry and Material Science of Photonics*, Science Press, Beijing, 2001.
38 (*a*) A. D. Joran, B. A. Leland, P. M. Felker, A. H. Zewail, J. J. Hopfield and P. B. Dervan, *Nature*, 1987, **327**, 508; (*b*) H. Zhang, M.-H. Zhang and T. Shen, *J. Photochem. Photobiol., A*, 1997, **103**, 63.
39 C. Laurence, P. Nicolet and M. T. Dalati, *J. Phys. Chem.*, 1994, **98**, 5807.
40 (*a*) P. G. Seybold and M. Gouterman, *J. Mol. Spectrosc.*, 1969, **31**, 1; (*b*) D. J. Quimby and F. R. Longo, *J. Am. Chem. Soc.*, 1975, **97**, 5111.
41 M. Holzinger, J. Abraham, P. Whelan, R. Graupner, L. Ley, F. Hennrich, M. Kappes and A. Hirsch, *J. Am. Chem. Soc.*, 2003, **125**, 8566.
42 (*a*) P. C. Hiemenz, *Principles of Colloid and Surface Chemistry*, Marcel Dekker, New York, 1986; (*b*) L. Jiang, *Photogr. Sci. Photochem.*, 1996, **14**, 77.
43 S. M. O'Flaherty, R. Murphy, S. V. Hold, M. Cadek, J. N. Coleman and W. J. Blau, *J. Phys. Chem. B*, 2003, **107**, 958.
44 (*a*) L. Vivien, P. Lancon, D. Riehl, F. Hache and E. Anglaret, *Carbon*, 2002, **40**, 1789; (*b*) S. Webster, M. Reyes-Reyes, X. Pedron, R. Lopez-Sandoval, M. Terrones and D. L. Carroll, *Adv. Mater.*, 2005, **17**, 1239; (*c*) N. Izard, P. Billaud, D. Riechl and E. Anglaret, *Opt. Lett.*, 2005, **30**, 1509.
45 L. Vivien, D. Riehl, J.-F. Delouis, J. A. Delaire, F. Hache and E. Anglaret, *J. Opt. Soc. Am. B*, 2002, **19**, 208.
46 (*a*) S. M. O'Flaherty, S. V. Hold, M. J. Cook, T. Torres, Y. Chen, M. Hanack and W. J. Blau, *Adv. Mater.*, 2003, **15**, 19; (*b*) A. Baev, O. Rubio-Pons, F. Gel'mukhanov and H. Ågren, *J. Phys. Chem. A*, 2004, **108**, 7406; (*c*) K. Sendhil, C. Vijayan and M. P. Kothiyal, *Opt. Mater.*, 2005, **27**, 1606.
47 W. Wu, S. Zhang, Y. Li, J.-X. Li, L.-Q. Liu, Y.-J. Qin, Z.-X. Guo, L.-M. Dai, C. Ye and D.-B. Zhu, *Macromolecules*, 2003, **36**, 6286.

